

Inverse magnetic catalysis in the (2+1)-flavor Nambu–Jona-Lasinio and Polyakov–Nambu–Jona-Lasinio models

M. Ferreira,^{1,2} P. Costa,¹ O. Lourenço,³ T. Frederico,² and C. Providência¹

¹*Centro de Física Computacional, Department of Physics,
University of Coimbra, P-3004 - 516 Coimbra, Portugal*

²*Instituto Tecnológico de Aeronáutica, 12.228-900, São José dos Campos, SP, Brazil*

³*Departamento de Ciências da Natureza, Matemática e Educação, CCA,
Universidade Federal de São Carlos, 13600-970, Araras, SP, Brazil*

(Dated: September 7, 2021)

The QCD phase diagram at zero chemical potential and finite temperature subject to an external magnetic field is studied within the three-flavor Nambu–Jona-Lasinio (NJL) model and the NJL model with the Polyakov loop. A scalar coupling parameter dependent on the magnetic field intensity is considered. The scalar coupling has been fitted so that the lattice QCD pseudocritical chiral transition temperatures are reproduced and in the limit of large magnetic field decreases with the inverse of the magnetic field intensity. This dependence of the coupling allows us to reproduce the lattice QCD results with respect to the quark condensates and Polyakov loop: due to the magnetic field the quark condensates are enhanced at low and high temperatures and suppressed for temperatures close to the transition temperatures and the Polyakov loop increases with the magnetic field.

PACS numbers: 24.10.Jv, 11.10.-z, 25.75.Nq / **Keywords:** PNJL, Polyakov loop, magnetic fields, transition temperatures

I. INTRODUCTION

In the last years, magnetized quark matter has attracted the attention of the physics community due to its relevance for heavy ion collisions at very high energies [1, 2], to the understanding of the first phases of the Universe [3] and for studies involving compact objects like magnetars [4].

In the presence of an external magnetic field, the behavior of quark matter is determined by the competition between two different mechanisms: the enhancement of the quark condensate because of the opening of the gap between the Landau states leading to the increase of low-energy contributions to the formation of the chiral condensate; and the suppression of the quark condensate due to the partial restoration of chiral symmetry. It was shown that in the region of low momenta relevant for chiral symmetry breaking there is a strong screening effect of the gluon interactions, which suppresses the condensate [5, 6]. In this region, the gluons acquire a mass M_g of the order of $\sqrt{N_f \alpha_s |eB|}$, due to the coupling of the gluon field to a quark-antiquark interacting state. In the presence of a strong enough magnetic field, this mass M_g for gluons becomes larger. This, along with the property that the strong coupling α_s decreases with increasing eB , $\alpha_s(eB) = (b \ln(|eB|/\Lambda_{QCD}^2))^{-1}$ with $b = (11N_c - 2N_f)/6\pi = 27/6\pi$, [6] leads to an effective weakening of the interaction between the quarks in the presence of an external magnetic field, and damps the chiral condensate.

The suppression of the quark condensate, also known as inverse magnetic catalysis (IMC), manifests itself on the decrease of the pseudocritical chiral transition temperature obtained in lattice QCD (LQCD) calcula-

tions with physical quark masses and an increase of the Polyakov field [5, 7, 8]. Recent results in two-flavor LQCD with dynamical overlap fermions in an external magnetic field also support the IMC scenario [9]. In particular, in [5] it is argued that the IMC may be a consequence of how the gluonic sector reacts to the presence of a magnetic field, and, it is shown that the magnetic field drives up the expectation value of the Polyakov field. The distribution of gluon fields changes as a consequence of the distortion of the quark loops in the magnetic field background. Therefore, the backreaction of the quarks on the gauge fields should be incorporated in effective models in order to describe the IMC.

Almost all low-energy effective models, at zero chemical potential, including the Nambu–Jona-Lasinio (NJL)-type models, find an enhancement of the condensate due to the magnetic field, and no reduction of the pseudocritical chiral transition temperature with the magnetic field [10]. However, a recent study using the Polyakov–Nambu–Jona-Lasinio (PNJL) [11] has shown that if the LQCD data [8] is fitted by making the pure-gauge critical temperature T_0 , a parameter of the PNJL model, eB dependent, the model is able to describe an IMC. Several recent studies [12–17] discuss the origin of the IMC phenomenon. In particular, the magnetic inhibition can be a possible explanation for the decreasing behavior of the chiral restoration temperature with increasing eB [13]; another mechanism to explain the IMC around the critical temperature as induced by sphalerons was proposed in [14].

The discussion above points out that the gluon distribution reacts to the magnetic background and suggests that the effective interaction between the quarks should get this dependence. With this motivation, we adopt a

running coupling constant of the chiral invariant quartic quark interaction in NJL and PNJL models with the magnetic field. The damping of the strength of the effective quartic interaction is built phenomenologically, keeping SU(3) flavor symmetry, under different assumptions inspired by lattice results for the quark condensate at finite temperature and magnetic field.

This paper is organized as follows. In Sec. II, we briefly present the PNJL model used in this work, the Polyakov loop potential, and the parametrizations chosen. In Sec. III, the importance of the running coupling in the (P)NJL models for magnetized quark matter is discussed. Also, the behavior of the condensates with temperature and the magnetic field intensity is compared with the LQCD results. Finally, in Sec. IV, the main conclusions are drawn.

II. MODEL AND FORMALISM

The PNJL Lagrangian with explicit chiral symmetry breaking, where the quarks couple to a (spatially constant) temporal background gauge field, represented in terms of the Polyakov loop, and in the presence of an external magnetic field is given by [18]

$$\mathcal{L} = \bar{q} [i\gamma_\mu D^\mu - \hat{m}_c] q + \mathcal{L}_{sym} + \mathcal{L}_{det} + \mathcal{U}(\Phi, \bar{\Phi}; T) - \frac{1}{4} F_{\mu\nu} F^{\mu\nu}, \quad (1)$$

where the quark sector is described by the SU(3) version of the NJL model which includes scalar-pseudoscalar and the 't Hooft six fermion interactions that models the axial $U_A(1)$ symmetry breaking [19], with \mathcal{L}_{sym} and \mathcal{L}_{det} given by [20],

$$\mathcal{L}_{sym} = \frac{G_s}{2} \sum_{a=0}^8 [(\bar{q}\lambda_a q)^2 + (\bar{q}i\gamma_5\lambda_a q)^2], \quad (2)$$

$$\mathcal{L}_{det} = -K \{ \det[\bar{q}(1 + \gamma_5)q] + \det[\bar{q}(1 - \gamma_5)q] \} \quad (3)$$

where $q = (u, d, s)^T$ represents a quark field with three flavors, $\hat{m}_c = \text{diag}_f(m_u, m_d, m_s)$ is the corresponding (current) mass matrix, $\lambda_0 = \sqrt{2/3}I$ where I is the unit matrix in the three-flavor space, and $0 < \lambda_a \leq 8$ denote the Gell-Mann matrices. The coupling between the (electro)magnetic field B and quarks, and between the effective gluon field and quarks is implemented *via* the covariant derivative $D^\mu = \partial^\mu - iq_f A_{EM}^\mu - iA^\mu$ where q_f represents the quark electric charge ($q_d = q_s = -q_u/2 = -e/3$), A_μ^{EM} and $F_{\mu\nu} = \partial_\mu A_\nu^{EM} - \partial_\nu A_\mu^{EM}$ are used to account for the external magnetic field and $A^\mu(x) = g_{strong} \mathcal{A}_a^\mu(x) \frac{\lambda_a}{2}$ where \mathcal{A}_a^μ is the SU_c(3) gauge field. We consider a static and constant magnetic field in the z direction, $A_\mu^{EM} = \delta_{\mu 2} x_1 B$. In the Polyakov gauge and at finite temperature the spatial components of the gluon field are neglected: $A^\mu = \delta_0^\mu A^0 = -i\delta_4^\mu A^4$. The trace of the Polyakov line defined by

$\Phi = \frac{1}{N_c} \langle \langle \mathcal{P} \exp i \int_0^\beta d\tau A_4(\vec{x}, \tau) \rangle \rangle_\beta$ is the Polyakov loop which is the order parameter of the \mathbb{Z}_3 symmetric/broken phase transition in pure gauge.

To describe the pure-gauge sector an effective potential $\mathcal{U}(\Phi, \bar{\Phi}; T)$ is chosen in order to reproduce the results obtained in lattice calculations [21],

$$\frac{\mathcal{U}(\Phi, \bar{\Phi}; T)}{T^4} = -\frac{a(T)}{2} \bar{\Phi} \Phi + b(T) \ln [1 - 6\bar{\Phi} \Phi + 4(\bar{\Phi}^3 + \Phi^3) - 3(\bar{\Phi} \Phi)^2], \quad (4)$$

where $a(T) = a_0 + a_1 (\frac{T_0}{T}) + a_2 (\frac{T_0}{T})^2$, $b(T) = b_3 (\frac{T_0}{T})^3$. The standard choice of the parameters for the effective potential \mathcal{U} is $a_0 = 3.51$, $a_1 = -2.47$, $a_2 = 15.2$, and $b_3 = -1.75$. The value of $T_0 = 210$ MeV is fixed in order to reproduce LQCD results (~ 170 MeV [22]),

We use as a regularization scheme, a sharp cutoff, Λ , in three-momentum space, only for the divergent ultra-violet sea quark integrals. The parameters of the model, Λ , the coupling constants G_s and K , and the current quark masses m_u and m_s are determined by fitting f_π , m_π , m_K and $m_{\eta'}$ to their empirical values. We consider $\Lambda = 602.3$, MeV, $m_u = m_d = 5.5$, MeV, $m_s = 140.7$ MeV, $G_s \Lambda^2 = 3.67$ and $K \Lambda^5 = 12.36$ as in [23]. The thermodynamical potential for the three-flavor quark sector Ω is written as

$$\Omega(T, \mu) = G_s \sum_{f=u,d,s} \langle \bar{q}_f q_f \rangle^2 + 4K \langle \bar{q}_u q_u \rangle \langle \bar{q}_d q_d \rangle \langle \bar{q}_s q_s \rangle + \mathcal{U}(\Phi, \bar{\Phi}, T) + \sum_{f=u,d,s} \left(\Omega_{vac}^f + \Omega_{med}^f + \Omega_{mag}^f \right) \quad (5)$$

where the flavor contributions from vacuum Ω_f^{vac} , medium Ω_f^{med} , and magnetic field Ω_f^{mag} [24] are given by

$$\Omega_{vac}^f = -6 \int_\Lambda \frac{d^3 p}{(2\pi)^3} \sqrt{p^2 + M_f^2} \quad (6)$$

$$\Omega_{med}^f = -T \frac{|q_f B|}{2\pi} \sum_{k=0}^{\infty} \alpha_k \int_{-\infty}^{+\infty} \frac{dp_z}{2\pi} (Z_\Phi^+(E_f) + Z_\Phi^-(E_f)) \quad (7)$$

$$\Omega_{mag}^f = -\frac{3(|q_f B|)^2}{2\pi^2} \left[\zeta'(-1, x_f) - \frac{1}{2}(x_f^2 - x_f) \ln x_f + \frac{x_f^2}{4} \right] \quad (8)$$

where $E_f = \sqrt{p_z^2 + M_f^2 + 2|q_f B|k}$, $\alpha_0 = 1$ and $\alpha_{k>0} = 2$, $x_f = M_f^2 / (2|q_f B|)$, and $\zeta'(-1, x_f) = d\zeta(z, x_f)/dz|_{z=-1}$, where $\zeta(z, x_f)$ is the Riemann-Hurwitz zeta function. At zero chemical potential the quark distribution functions $Z_\Phi^+(E_f)$ and $Z_\Phi^-(E_f)$ read

$$Z_\Phi^+ = Z_\Phi^- = \ln \{ 1 + 3\Phi e^{-\beta E_f} + 3\Phi e^{-2\beta E_f} + e^{-3\beta E_f} \} \quad (9)$$

once $\bar{\Phi} = \Phi$.

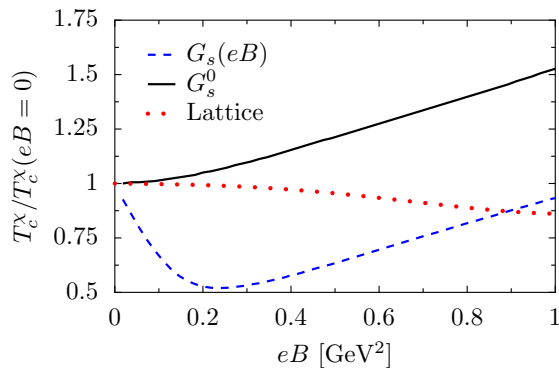


FIG. 1. The renormalized critical temperatures of the chiral transition ($T_c^X(eB=0) = 178$ MeV) as a function of eB in the NJL model with a magnetic field dependent coupling $G_s(eB)$ (blue dashed) and a constant coupling G_s^0 (black line), and the lattice results (red dots) [7].

III. RUNNING COUPLING IN THE (P)NJL MODEL FOR MAGNETIZED QUARK MATTER

A. NJL model

As already referred, the presence of an external magnetic field has two competing mechanisms: on one hand it enhances the chiral condensate due to the increase of low-energy contributions; on the other hand there is a suppression of the condensate because in the region of the low momenta relevant for the chiral symmetry breaking mechanism there is a strong screening effect of the gluon interactions [5, 6]. This suppression of the condensate, also known as IMC, manifests itself as the decrease of the pseudocritical chiral transition temperature obtained in LQCD calculations with physical quark masses [7, 8] and in the increasing of the Polyakov loop [5].

Within the NJL and PNJL models the inclusion of the magnetic field in the Lagrangian density allows us to describe the magnetic catalysis effect, but fails to account for the IMC. In the NJL model the quarks interact through local current-current couplings, assuming that the gluonic degrees of freedom can be frozen into point-like effective interactions between quarks. Therefore, we may expect that the screening of the gluon interaction discussed above weakens the interaction and which is translated into a decrease of the scalar coupling with the intensity of the magnetic field.

In [6], it was shown that the running coupling decreases with the magnetic field strength,

$$\alpha_s(eB) = \frac{1}{b \ln \frac{|eB|}{\Lambda_{QCD}^2}} \quad (10)$$

with $b = (11N_c - 2N_f)/6\pi = 27/6\pi$.

Consequently, in the NJL model the coupling G_s , which can be seen as $\propto \alpha_s$, must decrease with an increasing magnetic field strength.

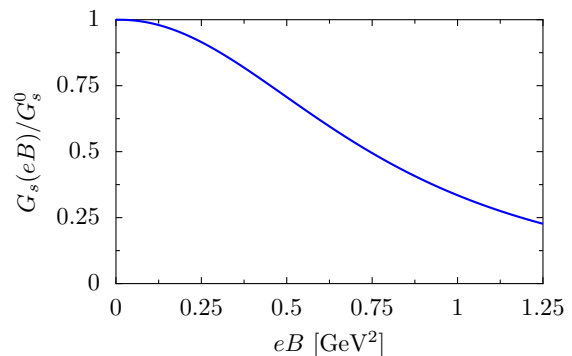


FIG. 2. The $G_s(eB)$ dependence calculated in the NJL model in order to reproduce the LQCD renormalized chiral transition temperature [7].

A first attempt to include the impact of the running coupling in the NJL model can be done by introducing the simple ansatz,¹

$$G_s(eB) = G_s^0 / \ln(e + |eB|/\Lambda_{QCD}^2). \quad (11)$$

In the limit case $eB \rightarrow \infty$, we obtain $G_s \rightarrow 0$, and for $eB \rightarrow 0$, we get $G_s \rightarrow G_s(eB=0) = G_s^0$. The pseudocritical temperatures for the chiral transitions $T_c^X = (T_u^X + T_d^X)/2$ (being T_u^X and T_d^X the transition temperatures for u and d quarks, respectively), are calculated using the location of the susceptibility peaks, $C_f = -m_\pi \partial \sigma_f / \partial T$, with $\sigma_f = \langle \bar{q}_f q_f \rangle(B, T) / \langle \bar{q}_f q_f \rangle(0, 0)$. The multiplication by m_π is only to ensure that the susceptibilities are dimensionless. Other methods to define the temperature transitions, such as those from the magnitude of the order parameters, are equally useful, see, for instance, Ref. [25]. The calculated chiral pseudocritical temperatures are shown in Fig. 1: when $G_s = G_s^0$ the model always shows a magnetic catalyzes, with increasing $T_c^X / T_c^X(eB)$ for all range of magnetic fields; when $G_s = G_s(eB)$, defined by Eq. (11), an IMC is seen until $eB \approx 0.3$ GeV², with the decrease of the pseudocritical temperature for low magnetic fields, but with the increase of $T_c^X / T_c^X(eB)$ for high eB values. Thus, with this simple ansatz, the model predicts an IMC at low eB and magnetic catalysis at high eB . This is in agreement with lattice results at high eB [26, 27]. It is worth noting that the logarithm behavior of the running coupling of QCD $\alpha_s(p^2)$, occurs for high momentum transfers $p \gg 1$ GeV. In this way, the $\alpha_s(eB) \propto \ln(|eB|/\Lambda_{QCD}^2)^{-1}$ behavior, may not be suitable for the low magnetic field range, $eB < 1$ GeV².

¹ When we were finalizing this article, the same idea was implemented in the SU(2) version of the NJL model [12]. However, in this paper, besides we are dealing with the SU(3) version of the model, we will fit $G_s(eB)$ to the LQCD results for the chiral transition pseudocritical temperature.

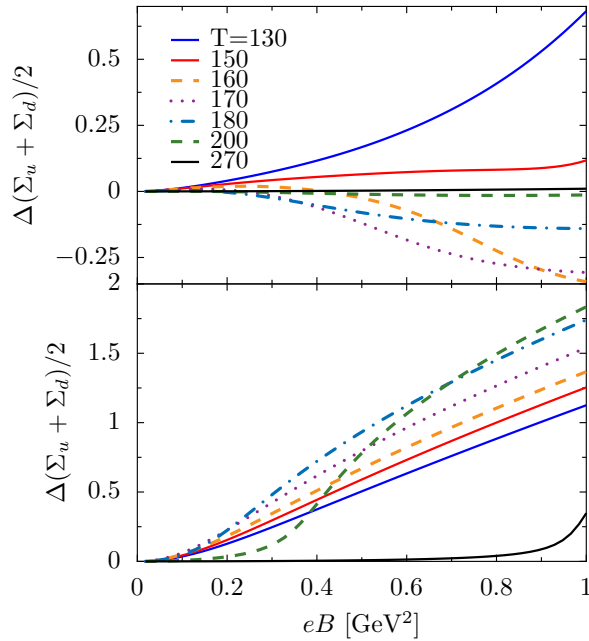


FIG. 3. The light chiral condensate $\Delta(\Sigma_u + \Sigma_d)/2$ as a function of eB , for several values of temperature in MeV, in the NJL model, with a magnetic field dependent coupling $G_s(eB)$ from Eq. (12) (top) and a constant coupling G_s^0 (bottom).

Since there is no LQCD data for $\alpha_s(eB)$ available, we will use another approach, in particular we will fit $G_s(eB)$ in order to reproduce $T_c^X(eB)$ obtained in LQCD calculations [7]. The resulting fit function of $G_s(eB)$, that reproduces the $T_c^X(eB)$ (see Fig. 7), is plotted in Fig. 2 and is written as

$$G_s(\zeta) = G_s^0 \left(\frac{1 + a\zeta^2 + b\zeta^3}{1 + c\zeta^2 + d\zeta^4} \right) \quad (12)$$

with $a = 0.0108805$, $b = -1.0133 \times 10^{-4}$, $c = 0.02228$, and $d = 1.84558 \times 10^{-4}$ and where $\zeta = eB/\Lambda_{QCD}^2$. We have used $\Lambda_{QCD} = 300$ MeV.

In [6], the authors have shown that in the presence of an external magnetic field and in the intermediate regime, corresponding to an energy scale below the magnetic field scale but larger than the dynamical quark mass, the gluon acquires a mass $M_g^2 \propto \alpha_s |eB|$. Thus in this limit of interest precisely at the chiral symmetry restoration transition, we have $G_s \propto \alpha_s/M_g^2 \propto 1/eB$. The above polynomial form insures that for $eB \rightarrow \infty$, G_s goes as $1/eB$.

In the following, we focus on the order parameter for the chiral transition, and, according to [8], we define the change of the light quark condensate due to the magnetic field as

$$\Delta\Sigma_f(B, T) = \Sigma_f(B, T) - \Sigma_f(0, T), \quad (13)$$

with

$$\Sigma_f(B, T) = \frac{2M_f}{m_\pi^2 f_\pi^2} [\langle \bar{q}_f q_f \rangle (B, T) - \langle \bar{q}_f q_f \rangle (0, 0)] + 1 \quad (14)$$

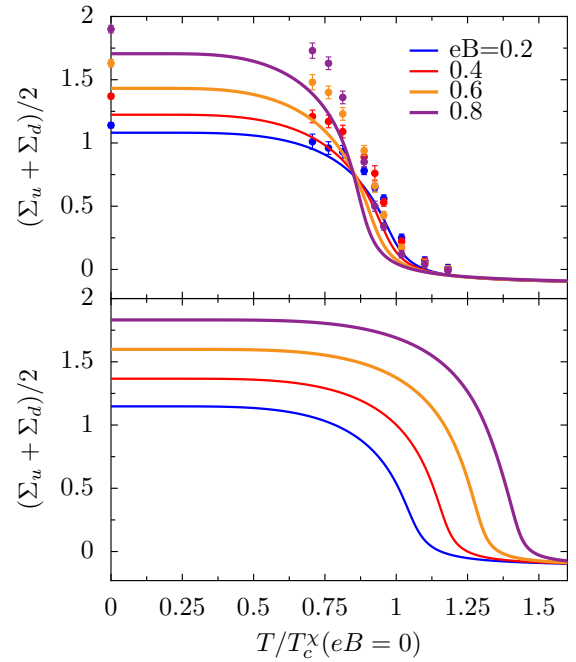


FIG. 4. The light chiral condensate $(\Sigma_u + \Sigma_d)/2$ as a function of temperature, for several values of eB in GeV^2 , in the NJL model, with a magnetic field dependent coupling $G_s(eB)$ from Eq. (12) compared with LQCD results [8] (top), and a constant coupling G_s^0 (bottom). The LQCD data was renormalized by $T_c^X(eB = 0) = 160$ MeV [8] and the NJL model results by $T_c^X(eB = 0) = 178$ MeV.

where the factor $m_\pi^2 f_\pi^2$ in the denominator contains the pion mass in the vacuum ($m_\pi = 135$ MeV) and (the chiral limit of the) pion decay constant ($f_\pi = 87.9$ MeV) in NJL model. The behavior of the quark condensates with the magnetic field is shown in Figs. 3-6.

In Fig. 3, the change of the renormalized condensate $\overline{\Delta\Sigma} = \Delta(\Sigma_u + \Sigma_d)/2$ as a function of the magnetic field intensity at several temperatures is shown for $G_s(eB)$ defined in Eq. (12) (top panel) and G_s^0 (bottom panel). The average of the light condensates calculated with $G_s(eB)$ shows the same behavior as LQCD calculations: at low and high temperatures the magnetic field enhances the condensates but at temperatures near the pseudocritical chiral transition temperature, the magnetic field suppresses the condensates. Using $G_s = G_s^0$, an enhancement is predicted at any temperature [11]: the magnetic catalysis is the result of an enhancement of the spectral density at low energies which increases the number of participants in the chiral condensate.

If $G_s = G_s^0$, and for $T < T_c^X(eB = 0)$, $\overline{\Delta\Sigma}$ increases with eB due to the magnetic catalysis effect, being its value even larger as the temperature is higher [11]. On the other hand, when $T > T_c^X(eB = 0)$ we are in the region where the partial restoration of chiral symmetry already took place. In this region there are two competitive effects: the partial restoration of chiral symmetry, that prevails at lower values of eB , making the condensate

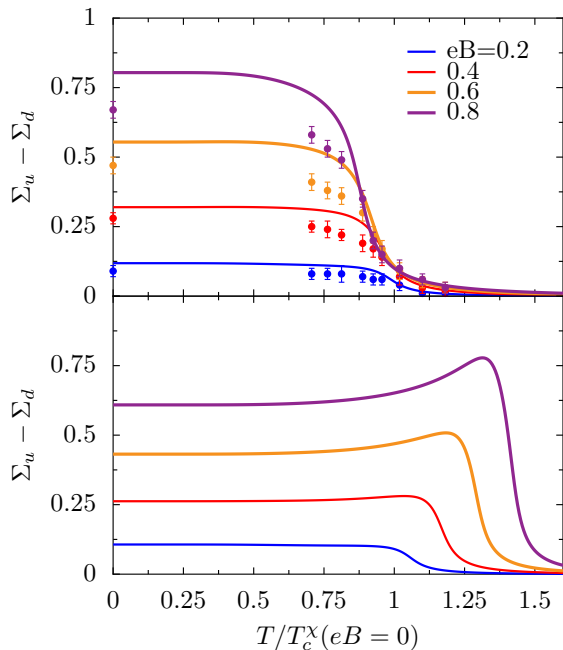


FIG. 5. The chiral condensate difference $\Sigma_u - \Sigma_d$ as a function of temperature, for several values of eB in GeV^2 , in the NJL model, calculated with a magnetic field dependent coupling $G_s(eB)$ [Eq. (12)] compared with LQCD results [8] (top), and a constant coupling G_s^0 (bottom). The LQCD data was renormalized by $T_c^\chi(eB=0) = 160$ MeV [8] and the NJL model results by $T_c^\chi(eB=0) = 178$ MeV.

average approximately zero, and the magnetic catalysis, that becomes dominant as the magnetic field increases. When the strength of the interaction decreases as eB increases, the coupling of a quark-antiquark pair interaction is weakened leading to the occurrence of an earlier partial restoration of chiral symmetry, so this effect is dominant preventing the magnetic catalysis to occur.

These same conclusions are obtained from Fig. 4 where the average light quark condensate is plotted as functions of T for several values of eB . The lattice results extracted from [8] have also been included in the top panel together with the results obtained with $G_s = G_s(eB)$ from Eq. (12). The qualitative agreement between both calculations is quite good, with the main features being reproduced by the NJL model. A very different behavior is obtained with a constant coupling G_s^0 , see Fig. 4 bottom, where the transition for larger values of eB occurs for larger temperatures.

In Figs. 5 and 6 the difference between light quark condensate are plotted, respectively, as a function of T for several values of eB , and as a function of eB for several temperatures. The lattice results from [8] have been included in Fig. 5 (top) together with the results for $G_s = G_s(eB)$. For comparison we also show the results for $G_s = G_s^0$ (bottom).

The bumps present in curves obtained with $G_s = G_s^0$ around the transition temperatures, a characteristic of

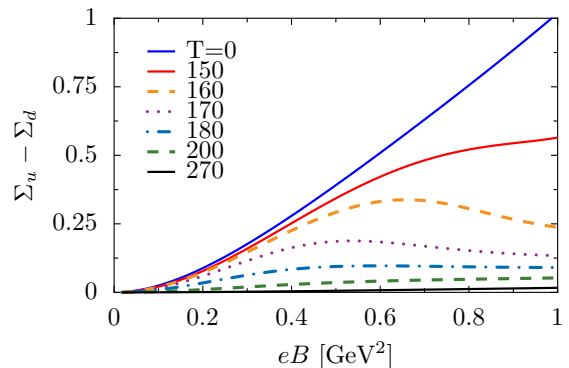


FIG. 6. The chiral condensate difference $\Sigma_u - \Sigma_d$ as a function of eB , for several values of temperature in MeV, in the NJL model, with a magnetic field dependent coupling $G_s(eB)$, Eq. (12).

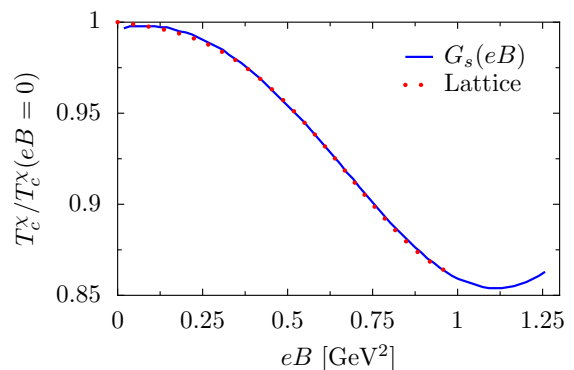


FIG. 7. The renormalized critical temperature of the chiral transition as a function of eB in the NJL model, with the magnetic field dependent coupling $G_s(eB)$ [Eq. (12)] (blue line) and LQCD results (red dots) [7].

the NJL with constant coupling, do not appear when $G_s(eB)$ is used, and a reasonable agreement with the LQCD results is achieved. As pointed out in [11], these bumps are the result of a stronger magnetic catalysis effect for the u quark, due to its larger electric charge, (the larger the magnetic field the larger the difference between u and d condensates, and the respective chiral transition temperatures), being this feature particularly strong close to the transition temperature, where the curves for stronger fields have a larger bump. When $G_s = G_s(eB)$, the effect due to the partial restoration of chiral symmetry will prevail over the magnetic catalysis due to a weaker interaction and, as already pointed out, the bumps will disappear in accordance with lattice results. In Fig. 6 the condensate difference $\Sigma_u - \Sigma_d$ is plotted as a function of eB for several temperatures and it is clearly seen that it always decreases with the temperature.

We next analyze the $T - eB$ phase diagram obtained within the NJL with a coupling dependent on the magnetic field. The parametrization $G_s(eB)$ was obtained

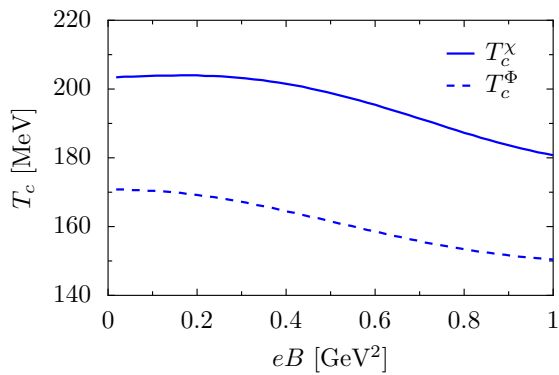


FIG. 8. The chiral and deconfinement transition temperatures as a function of eB in the PNJL, using the magnetic field dependent coupling $G_s(eB)$ [Eq. (12)].

using the available lattice results for the pseudocritical temperatures in the range $0 < eB < 1 \text{ GeV}^2$. The calculated pseudocritical temperatures are shown in Fig. 7 for a range of magnetic field intensities larger than the one used in the fit. For $eB \approx 1.1 \text{ GeV}^2$, the pseudocritical temperature starts to increase with eB . This behavior was also obtained in lattice calculations [26], which also predict magnetic catalysis at high values of eB . For $eB \approx 1.25 \text{ GeV}^2$ a chiral first order phase transition appears. The LQCD as well as the NJL results from Fig. 4 show that the average chiral condensate slope increases with increasing magnetic field. Thus, if this behavior persists for high magnetic fields, it is expected also from the LQCD results, that at some critical eB , the transition turns into a first order.

B. PNJL model

In the present section, we consider the PNJL model. In this model the the quark degrees of freedom are coupled to a Polyakov loop field which allows us to simulate a confinement-deconfinement phase transition at finite temperature. Several studies about the deconfinement and chiral symmetry restoration of hot QCD matter in an external magnetic field have recently been made [28–30]. Now, we will take for the scalar coupling parameter the same magnetic field dependent parametrization obtained in the previous section [Eq. (12)].

Next we discuss the effect of the magnetic field on the Polyakov loop and on the quark condensates within this model.

Some remarks are in order concerning the applicability of the PNJL model. It should be noticed that in this model, besides the chiral point-like coupling between quarks, the gluon dynamics is reduced to a simple static background field representing the Polyakov loop. As referred in Sec. II, we consider the parameter T_0 in the Polyakov loop $T_0 = 210 \text{ MeV}$, which takes into account the quark backreaction and reproduces the lattice decon-

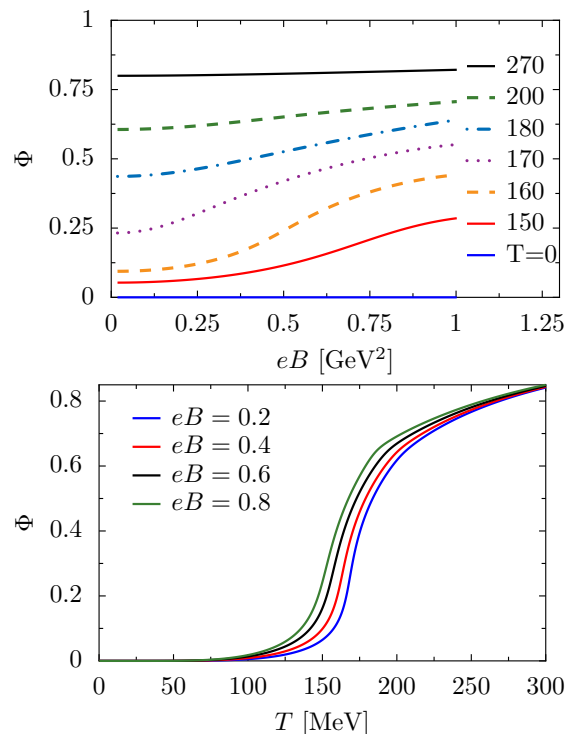


FIG. 9. The value of the Polyakov loop versus eB for several values of T (MeV) (top) and versus T for several values of eB in GeV^2 (bottom).

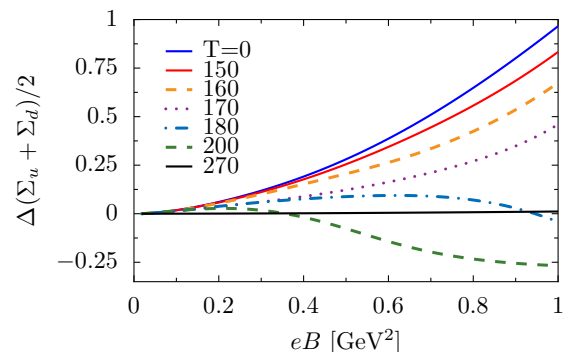


FIG. 10. The light chiral condensate $\Delta(\Sigma_u + \Sigma_d)/2$ as a function of eB , for several values of T in MeV, in the PNJL model.

finement pseudocritical temperature 170 MeV. As shown in the following, we obtain within the PNJL model several features discussed in the previous section, e. g. the deconfinement transition and the chiral transition pseudocritical temperatures are both decreasing functions with eB until a limiting magnetic field of $\sim 1 \text{ GeV}^2$, as in LQCD, see Fig. 8. Due to the existing coupling between the Polyakov loop field and quarks within PNJL, the $G_s(eB)$ does not only affect the chiral transition but also the deconfinement transition.

The effect of the magnetic field on the Polyakov loop is more clearly seen in Fig. 9 where Φ is plotted as a func-

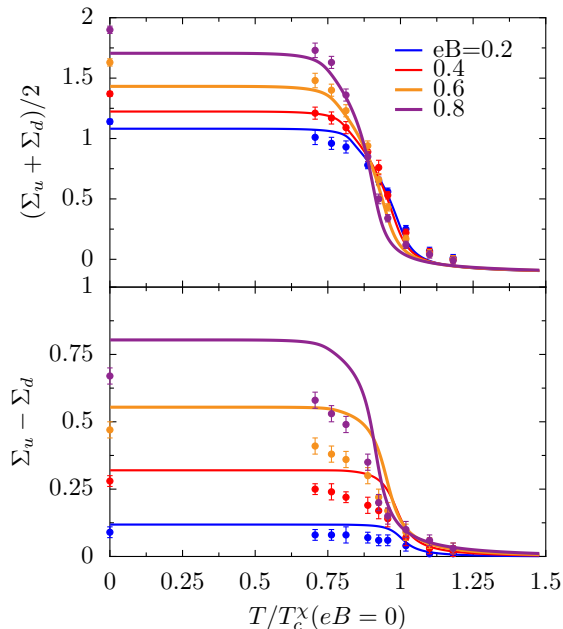


FIG. 11. The average $(\Sigma_u + \Sigma_d)/2$ (top) and the difference $(\Sigma_u - \Sigma_d)$ (bottom) of the light chiral condensates as a function of temperature, for several values of eB in GeV^2 , and the LQCD results [8]. The LQCD data was renormalized by $T_c^x(eB=0) = 160$ MeV [8] and the PNJL model results by $T_c^x(eB=0) = 203$ MeV.

tion of the magnetic field intensity for different values of the temperature (top), and as a function of temperature, for several magnetic field strengths (bottom). The suppression of the condensates achieved by the magnetic field dependence of the coupling parameter translates into an increase of the Polyakov loop. The effect of the magnetic field on Φ is stronger precisely for the temperatures close to the transition temperature, see Fig. 9 (top), in close agreement with the LQCD results [5].

In Fig. 10 we plot the average chiral condensate $\Delta(\Sigma_u + \Sigma_d)/2$ as a function of eB , for several temperatures. As in the LQCD [8], for temperatures smaller and higher than the transition temperatures, the model predicts a monotonously increase with eB , and for temperatures near the transition temperature, a nonmonotonic behavior is obtained. Thus, for $T \approx T_c^\Phi$, at magnetic field intensities higher than some pseudocritical value, the condensates are suppressed by the presence of the magnetic field.

In Fig. 11 the chiral condensate sum $(\Sigma_u + \Sigma_d)/2$ and the chiral condensate difference $\Sigma_u - \Sigma_d$ are plotted as a function of the temperature, renormalized by the pseudocritical temperature at zero magnetic field, for several magnetic field strengths and compared with the LQCD results from [8]. Just as already obtained for NJL, general features of the LQCD results are reproduced.

We observe that SU(3) symmetry of the pointlike effective interactions between quarks is assumed in the magnetic background, however the comparison with the

LQCD results for the difference in the quark condensates in Fig. 11 bottom, suggests that the up quark interaction is depleted with respect to the down quark one. That, seems reasonable as the effect of the magnetic field on the up quark is larger than in the down quark, and therefore the interaction between the up quarks should decrease with respect to the down quarks as the magnetic field increases. A more detailed calculation should account for magnetic SU(3) flavor breaking and it is postponed for a future work.

C. $G_s(eB)$ versus $T_0(eB)$

In Ref. [11] the possibility of describing the IMC effect within the models PNJL and entangled PNJL (EPNJL) by including a magnetic field dependent parameter $T_0(eB)$ in the parametrization of the Polyakov potential was studied. The main argument in favor was that back-reaction effects on the Polyakov loop due to the presence of a strong magnetic field should introduce screening effects leading to a reduction of the pseudocritical transition temperatures. A magnetic field dependent effective Polyakov potential could indeed describe the IMC effect but only within EPNJL. Neither the PNJL model [11] nor the two-flavor thermal quark-meson model [17] were able to obtain the IMC effect with a T_0 parameter dependent on the magnetic field. These results are in accordance with the results of the present work: in the EPNJL the coupling G_s depends on the Polyakov loop, and, therefore, at the crossover when the Polyakov loop increases the coupling G_s becomes weaker. This is shown in Fig. 12 top panel, where the coupling $G_s[\Phi(T)]$ of Ref. [11] is plotted for several temperatures (dashed curves) and, for comparison, the parametrization $G_s(eB)$ given in Eq. (12) and Fig. 2 is also included (full black line). It is interesting to realize that in the range $eB < 0.6$ GeV^2 , the curve obtained for $T = 210$ MeV, which is close to the deconfinement pseudocritical temperature ($T_c^\Phi = 214$ MeV), has a behavior in accordance with the results of the present work. Within the PNJL no IMC effect was obtained because the parameter $T_0(eB)$ does not affect the coupling G_s .

In Fig. 12 middle and bottom panels, we compare the results obtained in the present work with the ones of [11] for the pseudocritical temperatures and the Polyakov loop. In [11], the pseudocritical temperatures have a much flatter behavior at small values of the magnetic field reflecting the softer decrease of the coupling G_s for small values of the magnetic field shown in Fig. 12 top panel. Also, within the EPNJL with $T_0(eB)$ the difference between the pseudocritical temperatures T_c^X and T_c^Φ is much smaller because the Polyakov loop and the quark condensates are strongly coupled. For $eB=0$ these temperatures are almost coincident, but a finite strong magnetic field destroys this coincidence. PNJL does not have this feature and a $G_s(eB)$ coupling is not changing its normal behavior predicting different temperatures for T_c^X

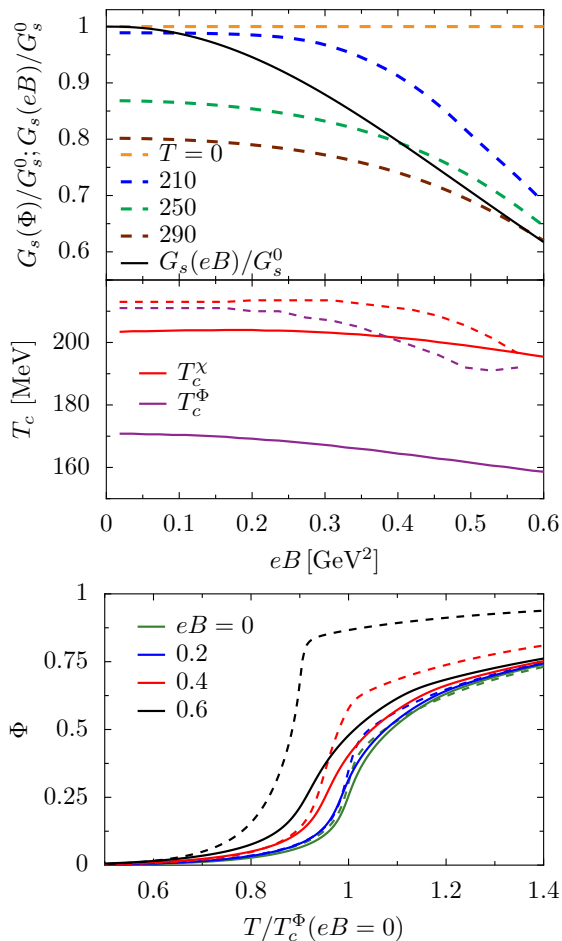


FIG. 12. Comparison between present work (full lines) and as results obtained within EPNJL with $T_0(eB)$ [11]. Top: The scalar coupling G_s versus the magnetic field, the black full line is the parametrization defined in (12) and plotted in Fig. 2; middle: the chiral and deconfinement pseudocritical temperatures versus the magnetic field; bottom: the Polyakov loop versus the temperature renormalized by the deconfinement pseudocritical temperature T_c^Φ for $eB = 0$, respectively, 171 MeV [PNJL with $G_s(eB)$] and 214 MeV [EPNJL with $T_0(eB)$].

and T_c^Φ . On the other hand, the effect of the parametrization $T_0(eB)$ on the Polyakov loop within EPNJL is much stronger than the one obtained in the present work, which is an indirect effect occurring due to the dependence of the quark distributions, Eq. (9), on the Polyakov loop.

IV. CONCLUSIONS

In the present work we study quark condensates and the QCD phase diagram at zero chemical potential and finite temperature subject to an external magnetic field within the NJL and PNJL models.

We have shown that recent results from LQCD, for quark matter in the presence of an external magnetic field, can be reproduced within NJL/PNJL models, if a magnetic field dependent coupling constant is used. A decreasing magnetic field dependent four quark coupling is essential, within effective quark models, to mimic the expected running of the coupling constant with the magnetic field strength and to incorporate the backreaction of the sea quarks in order to explain the IMC.

We have calculated the $G_s(eB)$ coupling constant in the NJL model, that reproduces the qualitative behavior of chiral pseudocritical temperature given by LQCD. All the qualitative results predicted by LQCD, can be reproduced using the calculated $G_s(eB)$ coupling: (a) the nonmonotonic behavior of the average condensate $\Delta(\Sigma_u + \Sigma_d)/2$ as a function of eB is obtained in the temperature region of the chiral transition; (b) the Polyakov loop increases with eB , and this increase is stronger for temperatures in the temperature region of the chiral transition; (c) the difference between the u and d quarks decreases monotonically with temperature, contrary to the prediction of the NJL and PNJL with constant couplings that predict an increase of this difference until the transition temperature. Furthermore, LQCD results suggest that the SU(3) symmetry of the pointlike effective interaction between quarks should be broken in the magnetic environment.

ACKNOWLEDGMENTS: This work was partially supported by Project No. PTDC/FIS/ 113292/2009 developed under the initiative QREN financed by the UE/FEDER through the program COMPETE: "Programa Operacional Factores de Competitividade", and by Grant No. SFRH/BD/51717/2011. We are also grateful to J. Moreira for useful discussions. T.F. thanks the Conselho Nacional de Desenvolvimento Científico e Tecnológico (CNPq) and T.F. and O.L. thank the Fundação de Amparo a Pesquisa do Estado de São Paulo (FAPESP).

[1] V. Skokov, A. Y. Illarionov, and V. Toneev, *Int. J. Mod. Phys. A* **24**, 5925 (2009); V. Voronyuk, V. Toneev, W. Cassing, E. Bratkovskaya, V. Konchakovski, and S. Voloshin, *Phys. Rev. C* **83**, 054911 (2011).
 [2] D. E. Kharzeev, L. D. McLerran and H. J. Warringa, *Nucl. Phys. A* **803**, 227 (2008).
 [3] T. Vachaspati, *Phys. Lett. B* **265**, 258 (1991); K. Enqvist

and P. Olesen, *Phys. Lett. B* **319**, 178 (1993).
 [4] R. C. Duncan and C. Thompson, *Astrophys. J.* **392**, L9 (1992); C. Kouveliotou *et al.*, *Nature (London)* **393**, 235 (1998).
 [5] F. Bruckmann, G. Endrodi and T. G. Kovacs, *J. High Energy Phys.* **04** (2013) 112.
 [6] V. A. Miransky and I. A. Shovkovy, *Phys. Rev. D* **66**,

- 045006 (2002).
- [7] G. S. Bali, F. Bruckmann, G. Endrödi, Z. Fodor, S. D. Katz, S. Krieg, A. Schäfer, and K. K. Szabó, *J. High Energy Phys.* **02** (2012) 044.
- [8] G. S. Bali, F. Bruckmann, G. Endrödi, Z. Fodor, S. D. Katz, and A. Schäfer, *Phys. Rev. D* **86**, 071502 (2012).
- [9] V. G. Bornyakov, P. V. Buividovich, N. Cundy, O. A. Kochetkov and A. Schäfer, arXiv:1312.5628 [hep-lat].
- [10] R. Gatto and M. Ruggieri, *Lect. Notes Phys.* **871**, 87 (2013); E. S. Fraga, *Lect. Notes Phys.* **871**, 121 (2013); E. S. Fraga, J. Noronha and L. F. Palhares, *Phys. Rev. D* **87**, 114014 (2013).
- [11] M. Ferreira, P. Costa, D.P. Menezes, C. Providência and N.N. Scoccola, *Phys. Rev. D* **89**, 016002 (2014).
- [12] R. L. S. Farias, K. P. Gomes, G. I. Krein and M. B. Pinto, arXiv:1404.3931 [hep-ph].
- [13] K. Fukushima and Y. Hidaka, *Phys. Rev. Lett.* **110** (2013) 031601.
- [14] J. Chao, P. Chu, and M. Huang, *Phys. Rev. D* **88** (2013) 054009.
- [15] K. Kamikado and T. Kanazawa, *J. High Energy Phys.* **03** (2014) 009.
- [16] J. O. Andersen, W. R. Naylor and A. Tranberg, *J. High Energy Phys.* **04** (2014) 187.
- [17] E. S. Fraga, B. W. Mintz and J. Schaffner-Bielich, *Phys. Lett. B* **731**, 154 (2014).
- [18] K. Fukushima, *Phys. Lett. B* **591**, 277 (2004); C. Ratti, M. A. Thaler, and W. Weise, *Phys. Rev. D* **73**, 014019 (2006).
- [19] T. Hatsuda and T. Kunihiro, *Phys. Rep.* **247**, 221 (1994); S.P. Klevansky, *Rev. Mod. Phys.* **64**, 649 (1992).
- [20] M. Buballa, *Phys. Rep.* **407**, 205 (2005).
- [21] S. Roessner, C. Ratti and W. Weise, *Phys. Rev. D* **75**, 034007 (2007).
- [22] Y. Aoki, S. Borsanyi, S. Durr, Z. Fodor, S. D. Katz, S. Krieg and K. K. Szabo, *J. High Energy Phys.* **06** (2009) 088.
- [23] P. Rehberg, S.P. Klevansky, and J. Hüfner, *Phys. Rev. C* **53**, 410 (1996).
- [24] D. P. Menezes, M. B. Pinto, S. S. Avancini, A. Perez Martinez and C. Providência, *Phys. Rev. C* **79**, 035807 (2009); D. P. Menezes, M. B. Pinto, S. S. Avancini and C. Providência, *Phys. Rev. C* **80**, 065805 (2009).
- [25] M. Dutra, O. Lourenço, A. Delfino, T. Frederico, and M. Malheiro, *Phys. Rev. D* **88**, 114013 (2013).
- [26] E. -M. Ilgenfritz, M. Muller-Preussker, B. Petersson and A. Schreiber, *Phys. Rev. D* **89**, 054512 (2014).
- [27] M. D'Elia, S. Mukherjee and F. Sanfilippo, *Phys. Rev. D* **82**, 051501 (2010).
- [28] P. Costa, M. Ferreira, H. Hansen, D. P. Menezes and C. Providência, *Phys. Rev. D* **89**, 056013 (2014).
- [29] M. Ferreira, P. Costa and C. Providência, *Phys. Rev. D* **89**, 036006 (2014).
- [30] W. -j. Fu, *Phys. Rev. D* **88**, 014009 (2013).